0026-895X/08/7403-662–672$20.00
MOLECULAR PHARMACOLOGY
Copyright © 2008 The American Society for Pharmacology and Experimental Therapeutics
Mol Pharmacol 74:662–672, 2008

Vol. 74, No. 3
49437/3379712
Printed in U.S.A.

Computational Discovery of Novel Low Micromolar Human Pregnane X Receptor Antagonists[S]

Sean Ekins, Vladyslav Kholodovych, Ni Ai, Michael Sinz, Joseph Gal, Lajos Gera, William J. Welsh, Kenneth Bachmann, and Sridhar Mani

Collaborations in Chemistry, Jenkintown, Pennsylvania (S.E.); Department of Pharmaceutical Sciences, University of Maryland, Baltimore, Maryland (S.E.); Department of Pharmacology, University of Medicine and Dentistry of New Jersey, Robert Wood Johnson Medical School, Piscataway, New Jersey (S.E., V.K., N.A., W.J.W.); Bristol-Myers Squibb Company, Wallingford, Connecticut (M.S.); Division of Clinical Pharmacology (J.G.) and Biochemistry and Molecular Genetics (L.G.), University of Colorado Denver, School of Medicine, Aurora, Colorado; Department of Pharmacology, The University of Toledo College of Pharmacy, Toledo, Ohio (K.B.); and Albert Einstein Cancer Center, Albert Einstein College of Medicine, Bronx, New York (S.M.)

Received June 3, 2008; accepted June 24, 2008

ABSTRACT

Very few antagonists have been identified for the human pregnane X receptor (PXR). These molecules may be of use for modulating the effects of therapeutic drugs, which are potent agonists for this receptor (e.g., some anticancer compounds and macrolide antibiotics), with subsequent effects on transcriptional regulation of xenobiotic metabolism and transporter genes. A recent novel pharmacophore for PXR antagonists was developed using three azoles and consisted of two hydrogen bond acceptor regions and two hydrophobic features. This pharmacophore also suggested an overall small binding site that was identified on the outer surface of the receptor at the AF-2 site and validated by docking studies. Using computational approaches to search libraries of known drugs or commercially available molecules is preferred over random screening. We have now described several new smaller antagonists of PXR discovered with the antagonist pharmacophore with in vitro activity in the low micromolar range [*S*-*p*-tolyl 3′,5-dimethyl-3,5′-biisoxazole-4′-carbothioate (SPB03255) (IC_{50}, 6.3 μM) and 4-(3-chlorophenyl)-5-(2,4-dichlorobenzylthio)-4*H*-1,2,4-triazol-3-ol (SPB00574) (IC_{50}, 24.8 μM)]. We have also used our computational pharmacophore and docking tools to suggest that most of the known PXR antagonists, such as coumestrol and sulforaphane, could also interact on the outer surface of PXR at the AF-2 domain. The involvement of this domain was also suggested by further site-directed mutagenesis work. We have additionally described an FDA approved prodrug, leflunomide (IC_{50}, 6.8 μM), that seems to be a PXR antagonist in vitro. These observations are important for predicting whether further molecules may interact with PXR as antagonists in vivo with potential therapeutic applications.

Our knowledge of ligand-protein interactions for some of the nuclear hormone receptors is in the nascent stages. This has downstream implications for understanding, predicting and modulating the potential xenobiotic and environmental molecule effects on transcription of key genes in human. For example, the pregnane X receptor (PXR; NR1I2; also known as SXR or PAR) regulates multiple genes, including the enzymes CYP3A4 (Bertilsson et al., 1998; Blumberg et al., 1998; Kliewer et al., 1998), CYP2B6 (Goodwin et al., 2001), and CYP2C9 as well as the transporter P-glycoprotein (ABCB1) (Synold et al., 2001) and others. There is a very broad structural diversity in the molecules that bind to human PXR from bile salts (Schuetz and Strom, 2001; Krasowski et al., 2005) to anticancer compounds (Mani et al., 2005; Ekins et al., 2007). Several X-ray crystal structures of the ligand binding domain (LBD) of PXR (Watkins et al., 2001, 2002, 2003a,b; Xue et al., 2007b) have determined that

S.E., N.A., V. K., and W.J.W. gratefully acknowledge the support for this work provided by the USEPA-funded Environmental Bioinformatics and Computational Toxicology Center (ebCTC), under STAR Grant number GAD R 832721-010. This work was supported in part by a grant from the Damon Runyon Cancer Research Foundation (15-02 to S.M).

S.E. and S.M. contributed equally to this work.

Article, publication date, and citation information can be found at http://molpharm.aspetjournals.org.

doi:10.1124/mol.108.049437.

[S] The online version of this article (available at http://molpharm.aspetjournals.org) contains supplemental material.

ABBREVIATIONS: PXR, pregnane X receptor; LBD, ligand binding domain; SRC-1, steroid receptor coactivator-1; AF-2, activation function-2; T-0901317, *N*-(4-(1,1,1,3,3,3-hexafluoro-2-hydroxy-propan-2-yl)phenyl)-*N*-(2,2,2-trifluoroethyl)benzenesulfonamide; ET-743, trabectedin; A-792611, (*S*)-1-[(1*S*,3*S*,4*S*)-4-[(*S*)-2-(3-benzyl-2-oxo-imidazolidin-1-yl)-3,3-dimethyl-butyrylamino]-3-hydroxy-5-phenyl-1-(4-pyridin-2-yl-benzyl)-pentylcarbamoyl]-2,2-dimethyl-propyl-carbamic acid methyl ester; DMEM, Dulbecco's modified Eagle's medium; FBS, fetal bovine serum; A771726, active α-cyanoenol metabolite of leflunomide.

it is a large, flexible, mostly hydrophobic site with some key polar residues. PXR also has key interactions with coactivators and corepressors (Johnson et al., 2006; Wang et al., 2006). Binding of the steroid receptor coactivator-1 (SRC-1) to activation function-2 (AF-2) on the surface of PXR is crucial for stabilizing the receptor (Watkins et al., 2003). In addition, a study using homology modeling and molecular dynamics simulation has been used to assess the interaction of the corepressor silencing mediator for retinoid and thyroid receptors (SMRT) with PXR (Wang et al., 2006).

In contrast to other nuclear receptors, such as the androgen receptor (Bohl et al., 2004; Bisson et al., 2007) and thyroid hormone receptor (Schapira et al., 2003b), the majority of publications on PXR have focused primarily on agonists (e.g., those capable of inducing drug metabolism and transporter expression) with clinical implications for drug-drug interactions (Ung et al., 2007). Conversely, there have been very few attempts to address antagonism at PXR, which could be used to diminish agonist interactions that are unavoidable with some treatments, such as with anticancer therapies and macrolide antibiotics such as rifampicin (Mani et al., 2005). There have however been previous efforts to generate antagonists at the LBD using a crystal structure of PXR with T-0901317 (Xue et al., 2007a), but this proved to be quite difficult to achieve (Lemaire et al., 2007). Yet there is a growing list of large- and small-molecule PXR antagonists that includes ET-743 (IC_{50}, 2 nM; mol. wt., 761.84; Synold et al., 2001), some polychlorinated biphenyls (K_i, 0.6–24.5 μM; Tabb et al., 2004), ketoconazole (IC_{50}, ~20 μM; mol. wt., 531.43)(Huang et al., 2007), fluconazole and enilconazole (IC_{50}, ~20 μM; mol. wt., 306.27 and 297.18, respectively; Wang et al., 2007), sulforaphane (IC_{50}, 12 μM; mol. wt., 177.29)(Zhou et al., 2007), coumestrol (IC_{50}, 12 μM; mol. wt., 268.22; Wang et al., 2008) and the HIV protease inhibitor A-792611 (IC_{50}, ~2 μM; mol. wt., 804.46; Healan-Greenberg et al., 2008). The variability in mol. wt., size and affinity of the antagonists might be indicative of different sites or mechanisms of antagonism. It is also not inconceivable that many of the antagonists are binding the same site by possessing a portion of the required pharmacophore for binding.

We have recently shown that the antagonists ketoconazole (Huang et al., 2007), fluconazole, and enilconazole (Wang et al., 2007) inhibit the activation of PXR in the presence of paclitaxel and behave as weak agonists on their own. Ketoconazole has also been shown to inhibit the PXR-SRC-1 interaction indicative of binding to the AF-2 site, and site-directed mutagenesis data provided confirmation of the importance of this location (Wang et al., 2007). It was additionally proposed that ketoconazole behaved similarly to the histidine residue of SRC-1 in interacting at the AF-2 site (Wang et al., 2007). We have previously tested this hypothesis using computational methods to derive a pharmacophore for the three azole antagonists as well as docking these molecules into regions on the outer surface of PXR (Ekins et al., 2007). This enabled us to define the likely key features and location where these antagonists bind. The properties of the pharmacophore for this site showed an equal balance between hydrogen bond acceptor and hydrophobic features, differing from the predominantly hydrophobic pharmacophores for agonists. The antagonist binding site was also suggested to overlap with the AF-2 region. Docking ketoconazole into this site showed it occupied two of three subsites of the motif where SRC-1 interacts. Docking of ketoconazole also indicated that the entire molecule may not be important for interaction with PXR because the piperazine ring was predicted as solvent-exposed. In combination with the pharmacophore, it was therefore possible to identify the minimum requirements for a pocket that ketoconazole, fluconazole, and enilconazole fitted into, suggesting utility for computer-aided antagonist design (Ekins et al., 2007). Therefore, it is possible that whereas ET-743 is a very large high-affinity antagonist that may interact in the ligand binding pocket of PXR (Synold et al., 2001), azoles, which are generally much smaller, are suggested to interact at the AF-2 site on the PXR surface.

In the current study, we have further validated the previously published PXR antagonist pharmacophore and used it to search data bases of molecules for novel PXR antagonists that have undergone in vitro testing. We have also used the antagonist pharmacophore to predict whether known published human PXR antagonists are likely to fit into the proposed antagonist pocket. In addition, we have compared results from the pharmacophore and GOLD docking to assess whether either or both of these approaches are useful for PXR antagonist discovery. This represents the first computational modeling using ligand- and protein-based methods to our knowledge that has enabled the prospective discovery of new "drug-like" PXR antagonists verified in vitro.

Materials and Methods

Materials

The cell culture medium used is DMEM. Lipofectamine 2000, phosphate-buffered saline, heat-inactivated fetal bovine serum (FBS), trypsin-EDTA (0.25%), and penicillin-streptomycin were purchased from Invitrogen (Carlsbad, CA). Charcoal/dextran-treated FBS was purchased from Hyclone (Logan, UT). HepG2 cells were obtained from the American Type Culture Collection (Manassas, VA). Human PXR-pcDNA3 and luciferase reporter containing CYP3A4 promoter, CYP3A-Luc, were generated at Bristol-Myers Squibb. White TC-surface 384-well plates were purchased from PerkinElmer Life and Analytical Sciences (Waltham, MA). Luciferase substrate (Steady-Glo) was purchased from Promega (Madison, WI). Rifampicin, leflunomide, and warfarin were purchased from Sigma (St. Louis, MO). Ketoconazole was purchased from BIOMOL International (Plymouth Meeting, PA); sulforaphane, indomethacin, bestatin, rosmarinic acid and itraconazole were purchased from LKT Laboratories Inc. (St. Paul, MN). "SPB" compounds were purchased from Ryan Scientific Inc. (Mt. Pleasant, SC). Individual ketoconazole enantiomers were prepared as described previously (Dilmaghanian et al., 2004).

In Silico Modeling

Catalyst. The computational molecular modeling studies were carried out using Catalyst in Discovery Studio 1.7 and 2.0 (Accelrys, San Diego, CA) running on either a Centrino or Centrino Duo processor (Intel, Santa Clara, CA). Pharmacophore models attempt to describe the arrangement of key features that are important for biological activity and their generation has been widely described previously (Clement and Mehl, 2000; Ekins et al., 2007). The previously reported common features PXR antagonist pharmacophore for the equipotent (~10 μM) PXR antagonists enilconazole, ketoconazole and fluconazole (Huang et al., 2007) has been described previously (Ekins et al., 2007). Ketoconazole served as the template molecule to which the other two azoles were aligned using hydrophobic, hydrogen bond acceptor, hydrogen bond donor, and ring aromatic features (Ekins et al., 2007). We also generated a van der Waals shape around

the enilconazole structure to create a more restrictive shape/feature hypothesis. Molecule data bases provided with the Discovery Studio software, such as the MiniMaybridge, a subset of the Maybridge vendor data base (2000 molecules) was used for data base searching with this pharmacophore. Additional data bases listed below were created using structures in the MDL SDF format before conversion to a 3D Catalyst data base after generating up to 100 molecule conformations with the FAST conformer generation method within the maximum energy threshold of 20 kcal/mol. The SCUT data base (2004) consisted of 579 known drugs in clinical use in the United States selected from the *Clinician's Pocket Drug Reference* (Gomella and Haist, 2004). This data base has previously been used to search for substrates and inhibitors for the transporters P-glycoprotein (Chang et al., 2006a) and human peptide transporter (Ekins et al., 2005). The BIOMOL natural products data base contains 481 molecules and BIOMOL known bioactives data base contains 473 molecules that were also converted into separate Catalyst data bases. For the data base mapping, we used rigid fitting and restricted the maximum omitted features to zero (the maximum number of pharmacophore features not mapped by the molecule).

For molecules not retrieved from data bases, the structures were sketched in ChemDraw for Excel (CambridgeSoft, Cambridge, MA) and exported as sdf files. In Catalyst, the three-dimensional molecular structures were produced using up to 255 conformers with the "best" conformer generation method, allowing a maximum energy threshold of 20 kcal/mol for each conformer. Using the Ligand Pharmacophore Mapping protocol, the "Best Mapping" was performed with the "rigid fitting method" and maximum omitted features set to zero. However, for the coumestrols and sulforaphane, the maximum omitted features were increased to 2 as these were found to miss one or more feature. The quality of the molecule mapping to the pharmacophore is determined by the fit value, with a higher fit value representative of a better fit and dependent on the proximity of the features to pharmacophore centroids and the weights assigned to each feature.

Substructure Searching. The molecule SPB 03255 was used as a query for substructure searching using two data bases that contain information on commercially available molecules namely, ChemSpider (http://www.chemspider.com/) and eMolecules (http://emolecules.com/databases). The two-dimensional molecular structures of retrieved molecules of interest were converted to three-dimensional conformations in Catalyst (as described above) and fitted with the PXR antagonist pharmacophore as well as the PXR pharmacophore with the enilconazole shape/feature restriction.

Docking Antagonists to the Crystal Structure Using GOLD. Protein preparation for GOLD docking (Jones et al., 1997) was done in Sybyl 7.2 (Tripos Inc., St.Louis, MO). The larger fragment of chain A, Ser192-Gly433 from the Protein Databank entry 1NRL was chosen for protein site preparation. Water molecules, salt ions, ligands and coreceptor fragments were deleted. After addition of hydrogen atoms and assigning of the AMBER 02 ForceField charges to the protein, only hydrogen position energy optimization was performed. The resulting protein was saved in Tripos mol2 format and used later as a docking site in GOLD.

The 1NRL chain A was used for rigid docking in which the protein was fixed and only flexibility was allowed for ligands. Each ligand was set to dock 20 times. The previously described (Ekins et al., 2007). Docking site (AF-2 site) was defined around the atom on the protruding tip of SRC-1: x 3.582, y 16.389, z 21.454 with a radius of 5 Å.

Cell Culture, PXR Transactivation, and Cytotoxicity Assays

The assays used to determine PXR agonists and antagonists have been described previously in detail and the reader is also referred to these (Mani et al., 2005; Huang et al., 2007; Wang et al., 2007, 2008). Culture of HepG2 cells was performed in T175 flasks using DMEM containing 10% FBS. The transfection mixture contains 1 μg/ml PXR-pcDNA3 plasmid DNA, 20 μg/ml Cyp3A-Luc plasmid DNA, 90 μl/ml Lipofectamine 2000, and serum-free medium. After incubating at room temperature for 20 min, the transfection mixture (1 ml per flask) was applied to the cells in fresh medium (20 ml per flask), and flasks were incubated at 37°C (5% CO_2) overnight. After the transient transfection, cells were trypsinized and cryopreserved for long-term storage.

On the day of the experiment, vials of cryopreserved cells were thawed and then resuspended in fresh medium (DMEM containing 5% charcoal/dextran-treated FBS, 1% penicillin/streptomycin, 100 μM nonessential amino acids, 1 mM sodium pyruvate, and 2 mM L-glutamine). Fifty microliters of cell mixture (8×10^3 cells) was added to wells of white tissue-culture–treated 384-well plates containing either 0.5 μl of test compound alone or a mixture of test compound and rifampicin (10 μM) dissolved in 100% dimethyl sulfoxide.

The plates were incubated at 37°C (5% CO_2) for 24 h, then 5 μl of Alamar Blue reagent (Trek Diagnostics) was added to each well. Plates were then incubated for an additional 2 h at 37°C, 5% CO_2 and then 1 h at room temperature. Fluorescence was read at an excitation wavelength of 525 nm and emission wavelength of 598 nm. After the fluorescence is measured, 25 μl of luciferase substrate (Steady-Glo; Promega) was added to each well. The plates were incubated for 15 min at room temperature, after which the luminescence was read on a Viewlux (PerkinElmer Life and Analytical Sciences) plate reader. In addition, drug-induced cytotoxicity was assessed by the 3-(4,5-dimethylthiazol-2-yl)-2,5-diphenyltetrazolium assay in cancer cell lines (LS174T and SKOV3) as well as fibroblast cells (CRL) (Ekins et al., 2007; Estébanez-Perpiñá et al., 2007). Cells were exposed to a concentration range of the drug(s) for 48 h. These assays were repeated three separate times, each in triplicate.

Site-Directed Mutagenesis

A site-specific mutation was made using QuikChange II site-directed mutagenesis kit (Stratagene, La Jolla, CA) protocol for polymerase chain reaction using manufacturer guidelines. The following primers were used (underlines indicate mutated nucleotides): Q272H: forward, 5′-ttgcccatcgaggacCATatctccctgctg-3′; reverse, 5′-cagcagggagatATGgtcctcgatgggcaa-3′.

The mutation was generated using pSG5-PXR plasmid (a gift from Steve Kliewer, University of Texas Southwestern Medical Center at Dallas) as a template. XL-blue competent cells were used to transform the PCR product(s), and bacterial colonies were used to isolate plasmid DNA. The clone was sequenced to confirm and verify the mutation.

Transfection Assay

CV-1 and 293T cells were transfected with PXR and reporter plasmids as indicated and previously published (Wang et al., 2008).

Data Analysis

Rifampicin (10 μM), a well known agonist of PXR, is included in each plate as an internal standard and positive control. The data are then expressed as percentage activation (%Act), where the total signal is the signal from the 10 μM rifampicin, and the blank signal is that from the dimethyl sulfoxide vehicle: %Act = [(Compound signal − Blank signal)/(Total signal − Blank signal)] × 100%.

Compounds are tested at 10 concentrations (2.5 nM–50 μM, 1:3 serial dilution). For PXR activation, a plot of concentration versus percentage activation was generated for each compound tested. For the plot, concentrations of compound at which 50% activation occurs (EC_{50}) are reported. For PXR inhibition, where the cells are incubated with 10 μM rifampicin and a concentration of test compound, percentage inhibition (%Inh) was calculated (%Inh = 100 − %Act). Concentrations of compound at which 50% inhibition occurs (IC_{50})

are reported and represent the mean of duplicate measurements unless otherwise stated.

Results

Fitting Known PXR Antagonists to the Pharmacophore. Enilconazole was mapped to the previously reported pharmacophore for PXR antagonists (Ekins et al., 2007), and the van der Waals shape of the molecule was used to produce a shape/feature pharmacophore (Fig. 1A). An interesting observation while creating this hypothesis was that enilconazole does not seem to map to the central hydrogen bond acceptor, so it is possible that this is not a key interaction for all antagonists and represents instead a common feature in fluconazole and ketoconazole, the other two molecules used to derive the HIPHOP (common feature alignment) pharmacophore. Sulforaphane, coumestrol, and their analogs were fitted to the PXR antagonist pharmacophore (Fig. 1); in the case of the coumestrols (Fig. 1, B–D), these failed to map at least one feature, whereas sulforaphane missed two features (Fig. 1E), and the two isomers scored similarly (Table 1). Previously reported biphenyl PXR antagonists (Tabb et al., 2004) analyzed map to the hydrophobic features only, missing the hydrogen bond acceptors (Fig. 1F). The HIV protease inhibitor A-792611, recently identified as a PXR antagonist (Healan-Greenberg et al., 2008), fitted to all the pharmacophore features once the shape restriction was removed. However, there was a substantial amount of the molecule outside of the pharmacophore, which might indicate potential for unfavorable steric clashes with the protein or solvent exposure (Supplemental Fig. 1).

Azole PXR Antagonist Pharmacophore Data Base Searching. The PXR antagonist pharmacophore was used to search the SCUT data base of approximately 600 widely prescribed drugs to identify nonazole drug molecules as potential antagonists. This pharmacophore was initially found to be quite nonselective: several hundred hits were retrieved.

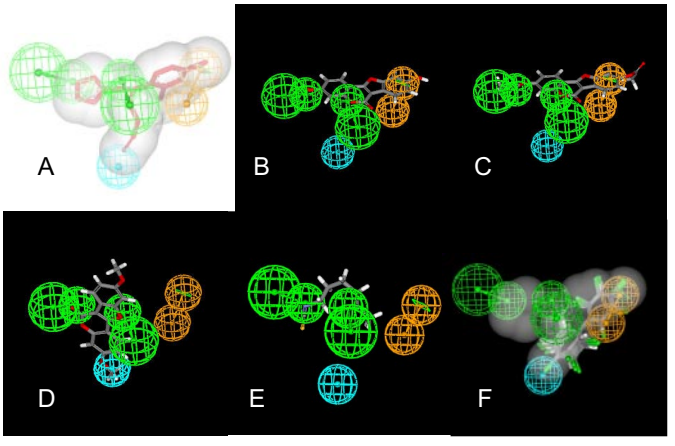

Fig. 1. The enilconazole shape/feature hypothesis for PXR antagonists and fit of coumestrol analogs, sulforaphane, and biphenyls. A, enilconazole was mapped to the previously described PXR antagonist pharmacophore, and a van der Waals surface was created around it. B, coumestrol. C, coumestrol diacetate. D, coumestrol dimethyl ether. E, sulforaphane. F, polychlorinated biphenyls mapped to the PXR antagonist pharmacophore. Note molecules B to F missed between one and two pharmacophore features, and therefore the pharmacophore fit score is not comparable with those for molecules in Table 1. Pharmacophore features: blue, hydrophobic; orange ring, aromatic/hydrophobic; green, hydrogen bond acceptor.

One approach to improve the selectivity of the pharmacophore was to add the van der Waals surface to enilconazole, one of the smaller azoles, when mapped to the pharmacophore (as described above), creating a shape/feature hypothesis (Fig. 1A). This shape/feature hypothesis was then used to search the SCUT data base and was found to be more restrictive, returning just 11 molecules (Supplemental Table 1) including four azoles (econazole, tioconazole, voriconazole, and fluconazole). The last of these was used in the initial pharmacophore model development. Indomethacin and warfarin were selected from this list based on their mapping to the pharmacophore and predicted fit (Table 1, Fig. 2A) and were tested in vitro. The "BIOMOL natural products" data base retrieved two hits (Supplemental Table 2); one of these, rosmarinic acid (Table 1, Fig. 2B) was tested in vitro. Searching the "BIOMOL known bioactives" data base retrieved five hits (Supplemental Table 3), and bestatin (Table 1, Fig. 2C) was selected for testing. Forty-nine hits were retrieved from the MiniMaybridge data base (Supplemental Table 4), and three of the highest scoring hits, including SPB03064 (Fig. 2D), SPB00574 (Fig. 2E) and SPB03255 (Fig. 2F), were selected for testing in vitro. In all cases, these molecules selected for testing seem to fit well to the pharmacophore.

Substructure Searching. Based on the greater than 90% structural similarity using the Tanimoto coefficient (ChemFinder; Cambridgesoft, Cambridge, MA) between fluconazole and itraconazole (Ekins et al., 2007) this latter molecule was also selected for in vitro testing. In addition, the molecule SPB03255 was used as a query for substructure searching using the internet chemistry data bases ChemSpider and eMolecules and suggested 18 structurally similar molecules (Table 2, Fig. 3, Supplemental Fig. 2) that were fitted to the PXR antagonist pharmacophore as well as the pharmacophore with shape. Several of the smaller molecules do not fit as well to the pharmacophore (no fit values), and these molecules were selected to delineate which part of the molecule are most important for antagonist activity. Leflunomide, which is similar in structure to SPB03255, is a US Food and Drug Administration-approved antirheumatic drug (Rozman, 2002) that was selected for testing based on its commercial availability.

Docking of Antagonists. Several of the known PXR antagonists were docked using GOLD and are shown in Fig. 3, including ketoconazole [GOLD score 50.98; Table 1 (Ekins et al., 2007), Fig. 4A], coumestrol (GOLD score 33.35; Fig. 4B), and newly discovered antagonists SPB03255 (GOLD score 38.22; Fig. 4C) and SPB06257 (GOLD score 47.26; Fig. 4D). Coumestrol, a flat structure, lies across the AF-2 site, whereas SPB03255 fills a part of the pocket in the same manner as the azoles, and SPB06257 extends out of the AF-2 pocket onto the surface. The sulforaphane isomers scored similarly (GOLD score 30; Table 1), whereas A-792611 had a slightly better fit (GOLD score 34.82). Interestingly, itraconazole scored similarly to ketoconazole (GOLD score 51.44; Table 1), and although there was no apparent direct correlation between antagonist activity and GOLD score, we did find that, in general, those scored the highest were likely to be more active in vitro. For example, of the four molecules tested with the highest GOLD score, three of them were found to be antagonists (Table 2). However, it should be noted that leflunomide was one of the lowest scoring molecules (Table 2),

and yet it had comparable activity to SPB03255, which scored higher (Table 1).

In Vitro Data. Ketoconazole was used as a positive control (as an example of a known antagonist) and has the approximately the same effect inhibiting the activation of rifampicin as in previous studies with paclitaxel (Table 1) (Huang et al., 2007; Wang et al., 2007). We have also tested the (+)-2*R*,4*S* and (−)-2*S*,4*R* enantiomers of ketoconazole and these seem to show no significant difference in their antagonistic effect (Table 1). Itraconazole was more potent than ketoconazole (IC_{50}, 8.96 μM). The previously shown antagonist sulforaphane was also tested as separate isomers and both were found to be more active (IC_{50}, 5.6 μM) than the previously published racemate and the antagonist coumestrol, both with reported IC_{50} values of 12 μM (Zhou et al., 2007; Wang et al., 2008). Rifampicin was used as a known PXR agonist, and the EC_{50} reported here is similar to those in other studies in HepG2 and other cell lines [EC_{50}, 400 nM (Hurst and Waxman, 2004)], such as CV-1 [EC_{50}, 700–852 nM (Chrencik et al., 2005); EC_{50}, 710 nM (Moore et al., 2000)].

From the initial PXR antagonist pharmacophore searching, several molecules were tested in vitro. Indomethacin, rosmarinic acid, warfarin, bestatin, and SPB03064 were inactive (Table 1), whereas SPB00574 was active (IC_{50}, 24.8 μM) and SPB03255 was more active (IC_{50}, 6.3 μM). None of these compounds was found to be a significant PXR agonist in vitro. Additional PXR antagonist analogs of SPB03255 were identified including SPB03256, SPB06061, SPB06257, and SPB02372. However, SPB03213, SPB03254, SPB03211, and SPB03663 were found to be selective agonists (Table 2 and Supplemental Fig. 2).

Site Directed Mutagenesis. Based on previous modeling predictions of the AF-2 contact residues with ketoconazole, the glutamine residue 272 was mutated to histidine (Q272H). The reasons for creating such a PXR mutant came from an ongoing yeast two-hybrid study in which several random mutants of PXR were generated and tested as a bait library using SRC-1 as prey. In this system, we picked several (>10) colonies of yeast that seemed to be immune from the inhibitory effects of ketoconazole. In all these colonies, there was a Q272H mutation that was present either alone or in combination with other LBD and non-LBD mutants (S. Mani, unpublished results). We decided to test the single Q272H mutant in a mammalian system to determine whether this mutant was 1) able to activate upon ligand (agonist) binding, 2) constitutively active, and/or 3) immune to the inhibitory effects of ketoconazole. Furthermore, an analog of ketoconazole (compound 3, Fig. 5) (Das et al., 2008) lacking the imidazole group but with a 2,4-difluoro substitution of the chloride atoms, resulted in a compound likely to lack contact with Gln272. PXR transcription studies in CV-1 cells were performed using the Q272H mutant of PXR cloned into a mammalian plasmid. The wild-type PXR plasmid was activated by rifampicin (2.3-fold) and was significantly inhibited by ketoconazole ($p < 0.0001$). The Q272H mutant of PXR was constitutively active, and rifampicin did not significantly augment basal activity. However, this mutant was not inhibited by ketoconazole (Fig. 5; $p = 0.181$). In contrast, compound 3 inhibited the Q272H mutant in the absence or presence of rifampicin ($p < 0.001$; $p < 0.003$).

Discussion

PXR Antagonist Pharmacophore Data Base Searching. We have described previously the first PXR antagonist pharmacophore that represents a region of the AF-2 domain on the outer surface of the protein and conforms to the site-directed mutagenesis and other in vitro data (Ekins et al., 2007). Although ketoconazole, enilconazole, and fluconazole were reported to be equipotent antagonists of PXR (Huang et al., 2007; Wang et al., 2007), we have also suggested that the entire ketoconazole structure may be unnec-

TABLE 1

Predicted fit of molecules to the PXR antagonist pharmacophore with shape restriction based on enilconazole, GOLD docking scores and biological data for PXR in agonist and antagonist modes

Molecular structures for indomethacin, rosmarinic acid, bestatin, SPB03064, SPB00574, and SPB03255 are shown in Figure 2. S.E.M. calculated from three sets of experiments, each performed in duplicate; those >50 were all >50 so S.E.M. = 0.

Molecule	Data Base Source	Catalyst Fit Value with Shape Restriction	GOLD Score (AF-2 site)	Agonist Mode PXR + DMSO EC_{50}	Antagonist Mode PXR + Rifampicin IC_{50}
				μM	
Itraconazole	Similarity to fluconazole using ChemFinder		51.44	>50[a]	8.96 ± 2.6
Indomethacin	SCUT and BIOMOL known bioactives	1.24	35.44	>50	>50
Warfarin	SCUT	1.32	41.15	>50	>50
Rosmarinic acid	BIOMOL natural products	1.60	35.64	>50	>50
Bestatin	BIOMOL known bioactives	0.61	38.30	>50	>50
SPB03064	MiniMaybridge	2.82	42.74	>50	>50
SPB00574	MiniMaybridge	2.14	43.47	>50	24.8 ± 3.2
SPB03255	MiniMaybridge	2.22	38.22	>50	6.3 ± 1.2
Rifampicin			9.15	0.78 ± 0.1	>50
(+)-2*R*,4*S*-Ketoconazole			51.52	>50	16.4 ± 0.3
(−)-2*S*,4*R*-Ketoconazole			51.80	>50	16.6 ± 0.3
(*S*)-Sulforaphane		(2.30)[b]	30.47	>50	5.64 ± 3.1
(*R*)-Sulforaphane		(1.90)[b]	30.42	>50	5.58 ± 3.6
Coumestrol		1.30	33.35	>50	12[c]

[a] >50 = inactive.
[b] Only maps two of four pharmacophore features using ligand pharmacophore mapping mode allowing rigid mapping and two features missed.
[c] Value previously published as an antagonist of SR12813, also antagonizes rifampicin mediated induction in human hepatocytes (Wang et al., 2008)

essary for antagonist activity. These three azole antagonists are proposed to partially mimic, displace, or interfere with the coactivator SRC-1 binding at the AF-2 site or close to this region, suggesting a therapeutic option for control of PXR-mediated transcription of target genes in cancer or to counter drug-drug interactions. The PXR antagonist pharmacophore also suggests a relatively small pocket with a balance of hydrogen bond acceptor and hydrophobic interactions (Ekins et al., 2007). We have indicated that computational methods could be useful to further explore the antagonist binding site by data base searching in a higher throughput fashion than feasible by random screening in vitro. The approaches taken in this study include use of the antagonist pharmacophore and docking molecules into the proposed antagonist site followed by in vitro verification. Precedent for such an approach using pharmacophores alone already exists to define new transporter inhibitors and substrates (Ekins et al., 2005; Chang et al., 2006b), although to our knowledge this is the first application of both ligand-based and structure-based (docking) methods to find PXR antagonists. Our hypothesis was that smaller molecules could be at least as active as ketoconazole.

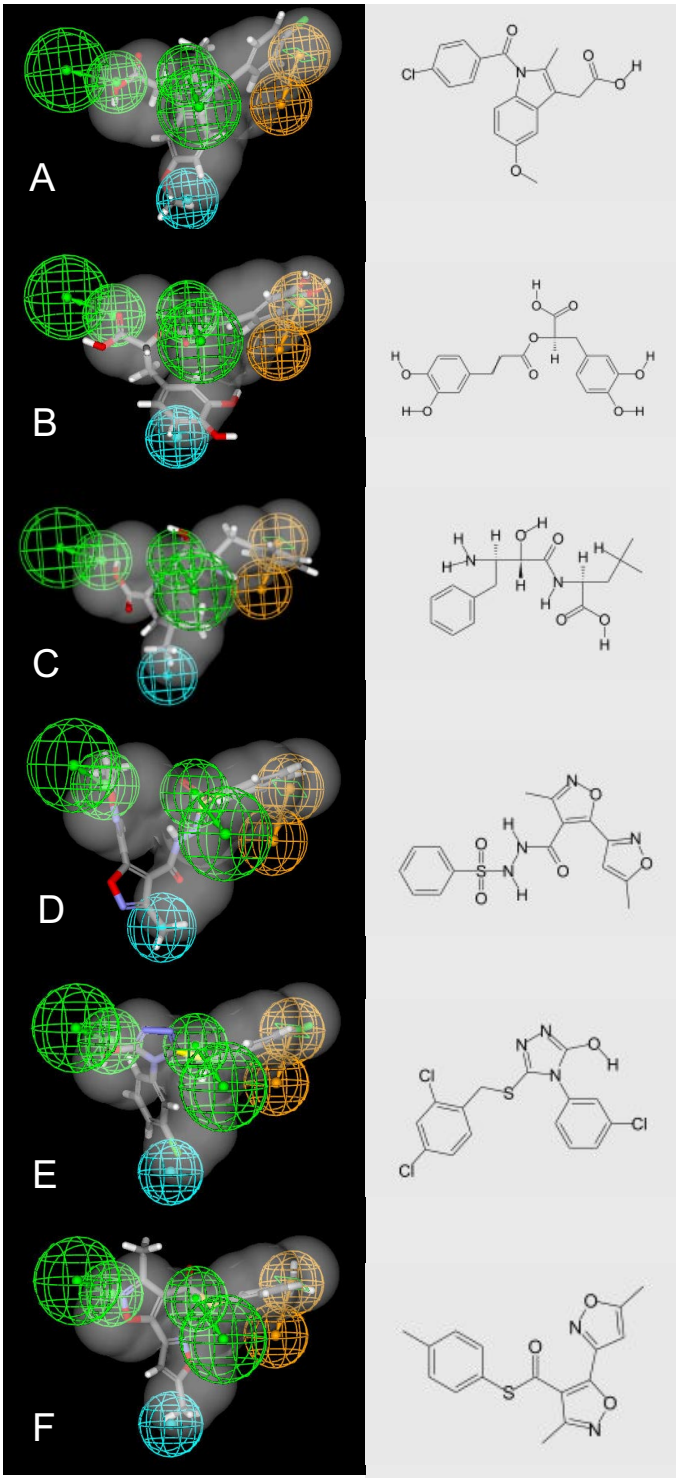

Fig. 2. Molecules derived from data base searching with the PXR antagonist pharmacophore (Ekins et al., 2007). A, indomethacin. B, rosmarinic acid. C, bestatin. D, SPB03064. E, SPB00574. F, SPB03255. Pharmacophore features: blue, hydrophobic; orange ring, aromatic/hydrophobic; green, hydrogen bond acceptor.

In the current study, we first fitted several diverse known PXR antagonists (Tabb et al., 2004; Wang et al., 2007; Zhou et al., 2007) to the pharmacophore to indicate coumestrol, sulforaphane, and A-792611 could potentially fit in the AF-2 site, based on the pharmacophore feature mapping (Fig. 1, Supplemental Fig. 1). The recently identified phytoestrogen coumestrol (Wang et al., 2008) possesses two hydroxyl groups as well as several other oxygen atoms that could serve as hydrogen bond acceptors. When the enilconazole van der Waals shape (Fig. 1A) is absent from the pharmacophore, the coumestrol molecule fits three features, both hydrogen bond acceptors, and the ring aromatic feature, but omits a hydrophobic feature (Fig. 1B). This suggests that coumestrol may bind the same site as the azoles, although the fit is perhaps suboptimal. Docking (Fig. 3) also indicates that coumestrol (Fig. 3C) may not fit ideally in this site. The two inactive analogs of coumestrol, the diacetate (Fig. 1, C and D) and coumestrol dimethyl ether, fit to the features (Fig. 1D); however, they extend beyond the enilconazole shape. In the case of the coumestrol dimethyl ether, the molecule is positioned 90° perpendicular to the original coumestrol mapping. Sulforaphane is a naturally occurring PXR antagonist (Zhou et al., 2007) that was found to only fit to the hydrogen bond acceptor features of the PXR antagonist pharmacophore (Fig. 1E). This provided weaker evidence that it could bind to the same external PXR surface site as the azoles, so it is possible that some pharmacophore features are more important than others. Likewise, we have found that an array of polychlorinated biphenyls (Tabb et al., 2004) may map only to the hydrophobic features of the pharmacophore (Fig. 1F). A-792611 could fit to all the pharmacophore features when the enilconazole shape was removed from the pharmacophore, which also suggests that a large percentage of the molecule could be outside of these pharmacophore features (Supplemental Fig. 1), much like the case with ketoconazole. The published experimental in vitro studies left open the possibility that A-792611 could bind outside of the PXR LBD (Healan-Greenberg et al., 2008). Given our pharmacophore analysis, it is a distinct possibility that all of the published PXR antagonists could be interacting at the AF-2 site like the azoles.

We have also used the PXR antagonist pharmacophore to search molecule data bases to discover novel antagonists. After our rather focused screening of four data bases, representing 3533 molecules, 67 hits were computationally retrieved (Supplemental Tables). We tested in vitro a selection

of these molecules based on their pharmacophore fit values and visual mapping to the pharmacophore features (Table 1), of which 2 initial molecules represented novel nonazole antagonists, namely SPB03255 (IC_{50}, 6.3 μM) and SPB00574 (IC_{50}, 24.8 μM; Fig. 2). SPB03255 and SPB00574 also scored highly based on the pharmacophore fit (Table 1). One high-scoring compound inactive in vitro (a false positive), SPB03064, contains an N-N bond that is possibly unstable during the incubation period in vitro. Indomethacin, bestatin, warfarin, and rosmarinic acid were also false positives and represent larger molecules that are lower scoring in terms of fit to the pharmacophore features and may not fit in the antagonist site as well. These inactive molecules may be useful to refine the pharmacophore in future. It is also interesting to note that the antagonist SPB00574 (Fig. 2E) is similar in structure to C2BA-6 (differing in a chlorine-substituted ring at the hydroxyl and other chlorine substitutions elsewhere), which was previously reported as a PXR agonist (EC_{50}, 1.89 μM) (Lemaire et al., 2007). In our study, SPB00574 did not seem to show appreciable PXR agonist activity.

One of the novel antagonists, SPB03255 was used as a foundation for substructure searching of two very large data bases to generate a structure activity relationship around this lead molecule. The chemistry data bases ChemSpider and eMolecules contained approximately 20×10^6 and 7×10^6 molecules, respectively, at the time of use, and enabled us to retrieve 18 molecules that were structurally similar to SPB03255. These molecules (Table 2, Supplementary Fig. 2) were also scored with the PXR antagonist pharmacophore, suggesting that several of the molecules had Catalyst fit scores similar or higher than the original molecule. We also discovered that SPB03213, SPB03254, SPB03211, and SPB03663 were selective PXR agonists in vitro (Table 2 and Supplemental Fig. 2). Three of these had a distinctly different substitution of the phenyl ring with chlorine, compared with the antagonist molecules with chlorine substitutions (Fig. 3). This is reminiscent of biphenyl compounds, some of which were antagonists, where it was hypothesized that the arrangement of the chlorines in a square or triangle pattern was a predictor of antagonism (Tabb et al., 2004). In this current study, hydrophobicity on the phenyl ring of the SPB compounds is mainly achieved with methyl or trifluoromethyl groups and the positioning is important. These relatively small PXR antagonists may of course flip inside the AF-2 site and so it is quite difficult to definitively locate potential ligand-protein interactions. It is also of interest that the antirheumatic compound leflunomide (IC_{50}, 6.8 μM) possesses a substructure similar to these active SPB compounds, although it possesses an amide linker. Leflunomide has also previously been reported to undergo N-O bond cleavage to the α-cyanoenol metabolite A771726 (Kalgutkar et al., 2003). which achieves median steady-state unbound plasma concentrations of approximately 1.1 μM (Chan et al., 2005). It is noteworthy that both leflunomide and A771726 mapped to the PXR antagonist pharmacophore with fit scores of 2.76 and 1.87, respectively, suggesting that both leflunomide and A771726 could behave as PXR antagonists (Supplemental Fig. 3). Future work will evaluate whether we are observing the PXR antagonist effect via the metabolite.

Docking of Molecules into the AF-2 Antagonist Site. We used a validated method for docking molecules into the AF-2 site, namely GOLD (Jones et al., 1997; Evers and Klabunde, 2005; Evers et al., 2005) and found that several molecules tested initially (Table 1) scored from 35 to 45 [lower than ketoconazole (Gold score 51)] and did not correlate with the in vitro activity. Itraconazole scored similarly to ketoconazole and was more active in vitro. We also tested two ketoconazole enantiomers (2*R*,4*S* and 2*S*,4*R*) and found them to have identical docking scores and in vitro activity. Previously modest enantioselective differences were shown for the same two ketoconazole enantiomers as inhibitors of CYP3A4 mediated testosterone and methadone metabolism (Dilmaghanian et al., 2004). In contrast, we found the docking scores of the 2*R*,4*R* enantiomer had a higher docking score of 56.45 and the 2*S*,4*S* enantiomer had a lower docking score of 49.24.

TABLE 2

Predicted and observed results using the PXR antagonist pharmacophores

GOLD docking scores and biological data after using the antagonist lead SPB03255 for substructure searching with ChemSpider and eMolecules. Docking scores in bold were the highest in the molecules tested in vitro. All molecule structures are shown in Figure 3 and Supplemental Figure 2.

Molecule	Catalyst Shape Fit		Catalyst Hypo Fit Only	GOLD Score (AF-2 site)	Agonist Mode PXR + DMSO EC_{50}[a]	Antagonist Mode PXR + RIF IC_{50}[a]
	Rigid	Flexible				
					μM	
SPB03256	0.71	1.62	2.11	**40.80**	>50	6.21
SPB03254	1.76	1.49	1.76	**43.24**	5.23	>50
SPB06061	—	—	0.62	37.54	>50	5.22
SPB03259	—	—	0.59	36.80	>50	>50
SPB03211	0.7	1.43	1.81	36.76	13.59	>50
SPB03213	—	—	1.7	36.65	1.71	>50
SPB03214	1.68	2.89	1.76	36.22	>50	>50
SPB03215	—	1.37	1.62	33.64	>50	>50
SPB03650	1.62	3.01	1.93	40.84	N.T.	N.T.
SPB03651	—	—	—	35.81	>50	>50
SPB03212	—	—	—	33.09	N.T.	N.T.
SPB03663	—	—	—	37.55	16.83	>50
Pubchem- 3169346	—	2.26	0.72	39.81	N.T.	N.T.
SPB06257	—	2.66	2.05	**47.26**	>50	16.42
SPB02372	—	—	1.44	**42.16**	>50	5.82
SPB06166	—	—	—	38.52	N.T.	N.T.
SPB06259	1.1	2.72	1.95	44.88	N.T.	N.T.
Leflunomide	—	—	—	31.00	>50	6.80

—, no fit; N.T., not tested.

[a] Data represents single runs in duplicate.

To date, we have not tested these latter two enantiomers in vitro. (*S*)-and (*R*)-Sulforaphane isomers were also similarly active with almost identical docking scores. Other known antagonists, coumestrol and A-792611, had docking scores from 30 to 34.8, which are low (Table 1), although visualizing coumestrol suggested it could fit in the AF-2 site. Our docking scores for the compounds that were selected for testing were generally higher in the most active molecules, in the 40 to 47 range. Docking may therefore be a useful addition to pharmacophores for filtering molecules for optimization.

Several groups have developed relatively simple approaches for guiding molecule optimization in drug discovery based on "ligand efficiency," which normalizes the binding affinity at the target with properties such as molecular weight, number of heavy atoms, or polar surface area (Hopkins et al., 2004; Abad-Zapatero and Metz, 2005; Reynolds et al., 2008). When we consider the PXR antagonists from Tables 1 and 2 compared with ketoconazole, the smallest molecules, such as sulforaphane and leflunomide, have the highest efficiency when measured by any of the three indices (Table 3). Coumestrol has similar efficiency for binding but not for the surface-binding index, because of its high polar surface area. Leflunomide and all of the SPB molecules have approximately 2-fold higher ligand and surface-binding efficiencies than ketoconazole, which is perhaps not surprising given their smaller size. When we consider the ligand efficiency versus heavy atom count (no hy-

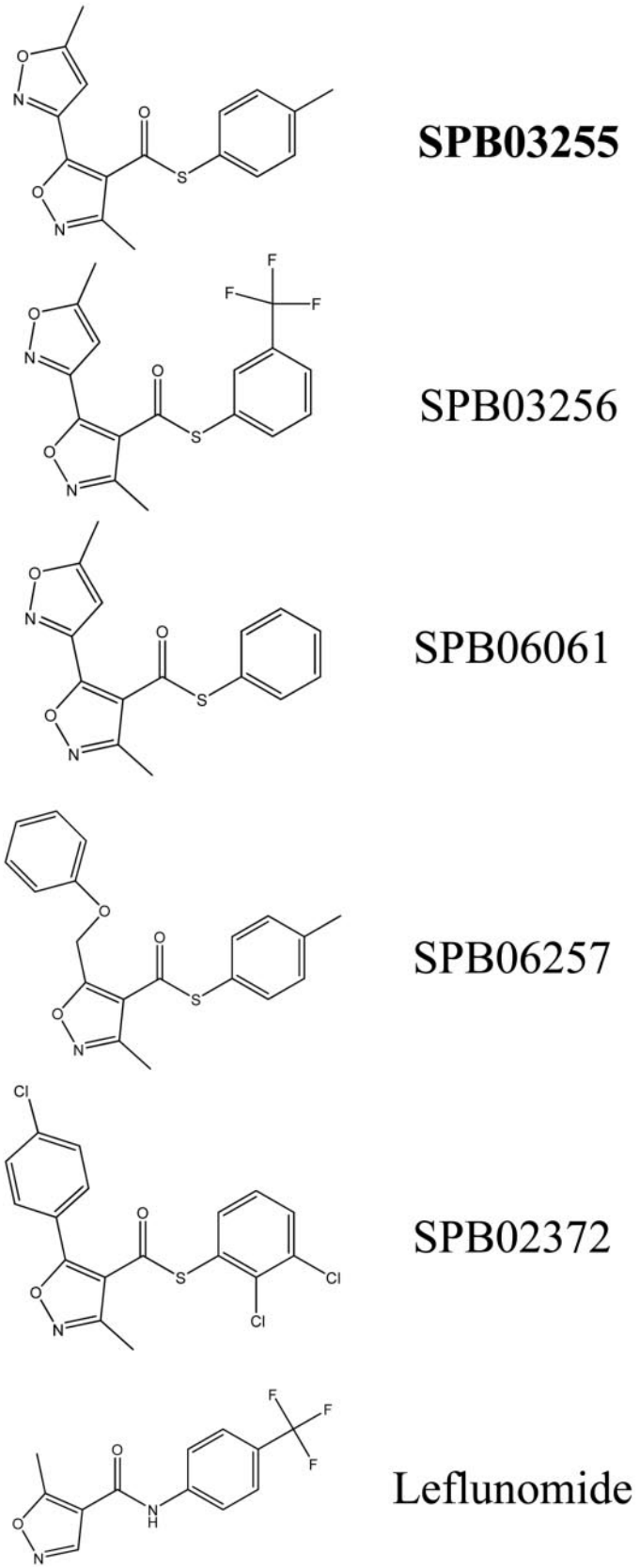

Fig. 3. SPB03255 and structural analogs showing PXR antagonist activity.

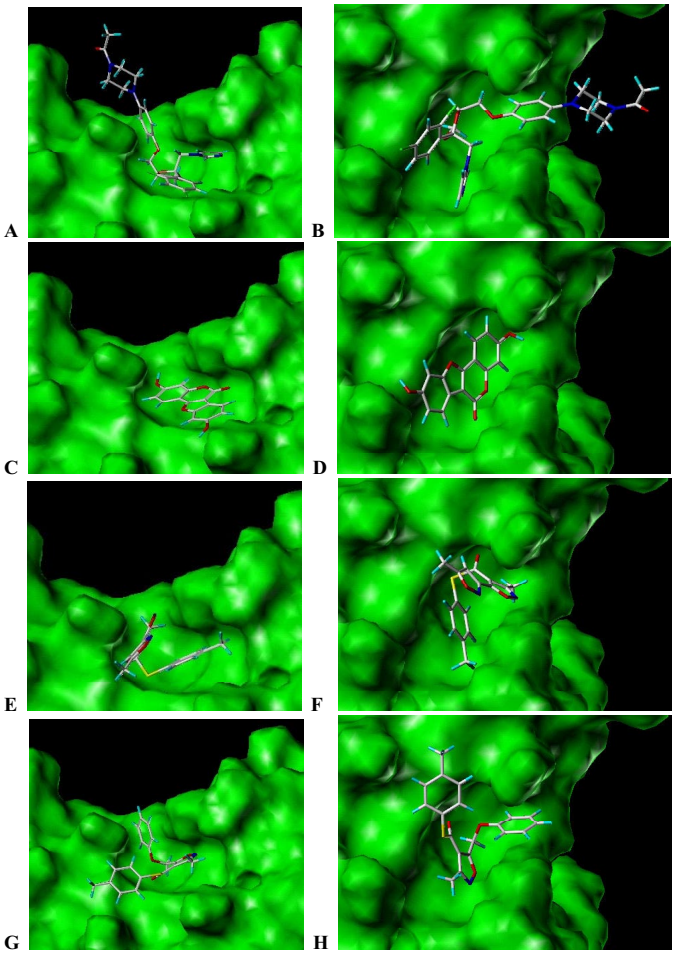

Fig. 4. Docking of PXR antagonists in the AF-2 antagonist site. A, side view of ketoconazole. B, front view of ketoconazole. C, side view of coumestrol. D, front view of coumestrol. E, side view of SPB03255. F, front view of SPB03255. G, side view of SPB06257. H, front view of SPB06257.

drogens) in Table 3, there is an exponential decrease in efficiency between 10 and 20 heavy atoms (data not shown), which is in line with observations of others for much larger data sets across different targets (Reynolds et al., 2008). Such calculated indices may therefore be useful when assessing and comparing future molecules as PXR antagonists.

Site Directed Mutagenesis. Previous site-directed mutagenesis studies had suggested that ketoconazole was bind-

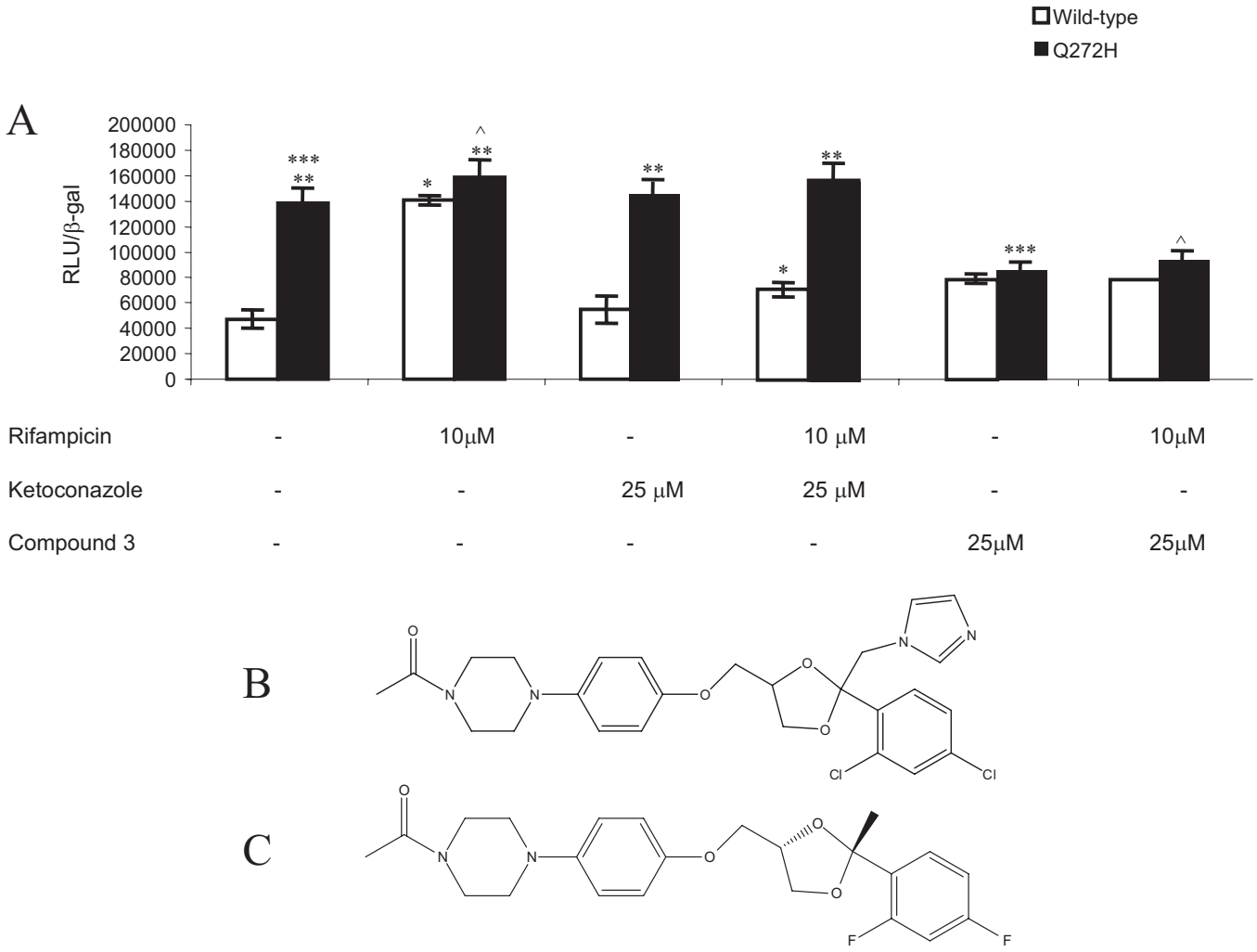

Fig. 5. Analysis of the single Q272H mutant in a mammalian system. A, PXR transcription studies in CV-1 cells were performed using the Q272H mutant of PXR cloned into a mammalian plasmid. The wild-type PXR plasmid was activated by rifampicin (2.3-fold) and was significantly inhibited by ketoconazole ($p < 0.0001$). The Q272H mutant of PXR was constitutively active and rifampicin did not significantly augment basal activity. However, this mutant was not inhibited by ketoconazole ($p = 0.181$). In contrast, the modified ketoconazole analog (compound 3) inhibited the Q272H mutant in the absence or presence of rifampicin ($p < 0.001$; $p < 0.003$). B, structure of ketoconazole. C, structure of compound 3 [1-(4-(4-(((2*R*,4*S*)-2-(2,4-difluorophenyl)-2-methyl-1,3-dioxolan-4-yl)methoxy)phenyl)piperazin-1-yl)ethanone].

TABLE 3

Calculated physicochemical properties and ligand efficiency indices

Properties calculated using Accelrys Discovery Studio 2.0.

Molecule	pIC_{50}	PSA	ALogP	Molecular Mass	HA	LE	BEI	SEI
		Å²		*Da*				
SPB06257	4.78	50.05	4.69	339.41	24	0.20	14.10	9.56
SPB02372	5.24	41.12	6.36	398.69	24	0.22	13.13	12.73
Leflunomide	5.17	53.93	2.16	270.21	19	0.27	19.12	9.58
Coumestrol	4.92	76.79	1.39	270.24	20	0.25	18.21	6.41
Itraconazole	5.05	96.69	6.43	705.63	49	0.10	7.15	5.22
SPB00574	4.61	48.69	5.94	386.68	23	0.20	11.91	9.46
Ketoconazole	4.78	67.41	3.61	531.43	36	0.13	9.00	7.10
Sulforaphane	5.25	28.62	1.16	177.29	10	0.52	29.61	18.34
SPB03255	5.20	64.93	3.88	314.36	22	0.24	16.54	8.01
SPB03256	5.21	64.93	4.34	368.33	25	0.21	14.14	8.02
SPB06061	5.28	64.93	3.39	300.33	21	0.25	17.59	8.14

PSA, polar surface area; HA, heavy atom count; LE, ligand efficiency [pIC_{50}/HA (Reynolds et al., 2008)]; BEI, binding efficiency index [pIC_{50}/molecular mass (kDa)]; SEI, surface-binding efficiency index [pIC_{50}/PSA (Abad-Zapatero and Metz, 2005)].

ing on the outer surface of PXR (Wang et al., 2007). The Q272H mutation undertaken in this study is in the AF-2 cleft and is conservative (glutamine to histidine). These two amino acids are isostructural with regard to polar atoms on glutamine. Based on crystal structure data (Watkins et al., 2003; Xue et al., 2007b) with the SRC-1 peptide, isostructural changes are unlikely to disrupt coactivator binding; thus, these mutants are active, especially upon ligand (agonist) binding. However, in our previous article (Ekins et al., 2007), we predicted that Gln272 is an important contact residue for the imidazole ring of ketoconazole in one binding orientation. Our data show, in fact, that substitution with the bulky histidine ring can block ketoconazole binding to PXR, whereas a ketoconazole analog compound 3 [Fig. 5, synthesis to be described elsewhere (Das et al., 2008)] that lacks the imidazole ring and substitutes the chlorines with fluorines, retains antagonism of the Q272H mutant (Das et al., 2008). These data validate a residue interaction prediction based on our previously published computational data (Ekins et al., 2007) and provide further confidence that these antagonists are likely to bind in the AF-2 site.

We have used the previously published human PXR antagonist pharmacophore to discover new PXR antagonists that were verified in vitro. In addition, we have used docking, an approach that has been widely applied elsewhere for virtual discovery of new leads for nuclear hormone receptors (Schapira et al., 2000, 2001, 2003a,b) as well as many other therapeutic targets (Leach et al., 2006; Bisson et al., 2007; Zhang et al., 2007). We found that some of the antagonists, such as ketoconazole and itraconazole, generally score well; this may be because the docking program picks up nonspecific van der Waals interactions of large molecules on the outer surface of the AF-2 site. The smaller antagonists discovered such as SPB03255 generally do not have very high docking scores. It would seem that using the PXR pharmacophore may therefore be a useful tool for rapid screening of molecule data bases and identifying potential antagonists that can be followed up with docking. These molecules in turn will need further preclinical assessment to ensure that they are likely to progress as potential clinical candidates (Ekins et al., 2007; Huang et al., 2007; Wang et al., 2007). Potential important applications of PXR antagonists include prevention of drug-drug interactions and potential changes in drug pharmacokinetics. We and others have shown that PXR activation can lead to cancer cell proliferation and drug resistance; therefore, blocking drug-induced PXR activation can mitigate antiapoptotic effects of certain xenobiotics (Chen et al., 2007; Gupta et al., 2008). PXR also induces P-glycoprotein at the blood-brain barrier, increasing drug efflux from the brain, and tightens this barrier (Bauer et al., 2004; Bauer et al., 2006). Interference with this could increase retention of drugs in the central nervous system when desired.

In summary, we have described several new smaller more efficient antagonists of PXR, to follow on from the initial azoles (such as ketoconazole) identified previously. These molecules have in vitro activity in the low micromolar range, which is similar to the sulforaphane isomers, and itraconazole. We have also used our computational pharmacophore and docking tools to suggest that most of the known PXR antagonists could also interact on the outer surface of PXR at the AF-2 domain, which is also supported by further site-directed mutagenesis work undertaken in this study with a ketoconazole analog that is lacking the imidazole group. We have also described for the first time that a U.S. Food and Drug Administration-approved prodrug, leflunomide, seems to be a PXR antagonist in vitro. Further studies will be important to describe the clinical relevance of this and other antagonists identified thus far, to suggest other analogs that may have applications in modulating PXR activity and downstream gene expression in vivo for cancer, pharmacokinetics, or drug resistance applications.

Acknowledgments

We gratefully acknowledge Dr. Maggie A.Z. Hupcey for support; Dr. Matthew D. Krasowski (University of Pittsburgh) for providing the BIOMOL sdf files; Dr. Sean Kim for support of the PXR transactivation assay; Accelrys (San Diego, CA) for making Discovery Studio Catalyst available; and the reviewers for their useful suggestions.

References

Abad-Zapatero C and Metz JT (2005) Ligand efficiency indices as guideposts for drug discovery. *Drug Discov Today* **10:**464–469.

Bauer B, Hartz AM, Fricker G, and Miller DS (2004) Pregnane X receptor up-regulation of P-glycoprotein expression and transport function at the blood-brain barrier. *Mol Pharmacol* **66:**413–419.

Bauer B, Yang X, Hartz AM, Olson ER, Zhao R, Kalvass JC, Pollack GM, and Miller DS (2006) In vivo activation of human pregnane X receptor tightens the blood-brain barrier to methadone through P-glycoprotein up-regulation. *Mol Pharmacol* **70:**1212–1219.

Bertilsson G, Heidrich J, Svensson K, Asman M, Jendeberg L, Sydow-Bäckman M, Ohlsson R, Postlind H, Blomquist P, and Berkenstam A (1998) Identification of a human nuclear receptor defines a new signaling pathway for CYP3A induction. *Proc Natl Acad Sci U S A* **95:**12208–12213.

Bisson WH, Cheltsov AV, Bruey-Sedano N, Lin B, Chen J, Goldberger N, May LT, Christopoulos A, Dalton JT, Sexton PM, et al. (2007) Discovery of antiandrogen activity of nonsteroidal scaffolds of marketed drugs. *Proc Natl Acad Sci U S A* **104:**11927–11932.

Blumberg B, Sabbagh W Jr, Juguilon H, Bolado J Jr, van Meter CM, Ong ES, and Evans RM (1998) SXR, a novel steroid and xenobiotic-sensing nuclear receptor. *Genes Dev* **12:**3195–3205.

Bohl CE, Chang C, Mohler ML, Chen J, Miller DD, Swaan PW, and Dalton JT (2004) A ligand-based approach to identify quantitative structure-activity relationships for the androgen receptor. *J Med Chem* **47:**3765–3776.

Chan V, Charles BG, and Tett SE (2005) Population pharmacokinetics and association between A77 1726 plasma concentrations and disease activity measures following administration of leflunomide to people with rheumatoid arthritis. *Br J Clin Pharmacol* **60:**257–264.

Chang C, Bahadduri PM, Polli JE, Swaan PW, and Ekins S (2006a) Rapid Identification of P-glycoprotein Substrates and Inhibitors. *Drug Metab Dispos* **34:**1976–1984.

Chang C, Ekins S, Bahadduri P, and Swaan PW (2006b) Pharmacophore-based discovery of ligands for drug transporters. *Adv Drug Deliv Rev* **58:**1431–1450.

Chen Y, Tang Y, Wang MT, Zeng S, and Nie D (2007) Human pregnane X receptor and resistance to chemotherapy in prostate cancer. *Cancer Res* **67:**10361–10367.

Chrencik JE, Orans J, Moore LB, Xue Y, Peng L, Collins JL, Wisely GB, Lambert MH, Kliewer SA, and Redinbo MR (2005) Structural disorder in the complex of human pregnane X receptor and the macrolide antibiotic rifampicin. *Mol Endocrinol* **19:**1125–1134.

Clement OO and Mehl AT (2000) HipHop: Pharmacophore based on multiple common-feature alignments, in *Pharmacophore Perception, Development, and Use in Drug Design* (Guner OF ed) pp 69–84, IUL, San Diego.

Das BC, Madhukumar AV, Kim S, Sinz M, Zvyaga TA, Power EC, Ganellin CR and Mani S (2008) Synthesis of novel ketoconazole derivatives as antagonists of the human pregnane X receptor (PXR; NR1I2; also termed SXR, PAR). *Bioorg Med Chem Lett*, in press.

Dilmaghanian S, Gerber JG, Filler SG, Sanchez A, and Gal J (2004) Enantioselectivity of inhibition of cytochrome P450 3A4 (CYP3A4) by ketoconazole: testosterone and methadone as substrates. *Chirality* **16:**79–85.

Ekins S, Chang C, Mani S, Krasowski MD, Reschly EJ, Iyer M, Kholodovych V, Ai N, Welsh WJ, Sinz M, et al. (2007) Human pregnane X receptor antagonists and agonists define molecular requirements for different binding sites. *Mol Pharmacol* **72:**592–603.

Ekins S, Johnston JS, Bahadduri P, D'Souza VM, Ray A, Chang C, and Swaan PW (2005) In vitro and pharmacophore based discovery of novel hPEPT1 inhibitors. *Pharm Res* **22:**512–517.

Estébanez-Perpiñá E, Arnold LA, Arnold AA, Nguyen P, Rodrigues ED, Mar E, Bateman R, Pallai P, Shokat KM, Baxter JD, et al. (2007) A surface on the androgen receptor that allosterically regulates coactivator binding. *Proc Natl Acad Sci U S A* **104:**16074–16079.

Evers A, Hessler G, Matter H, and Klabunde T (2005) Virtual screening of biogenic amine-binding G-protein coupled receptors: comparative evaluation of protein- and ligand-based virtual screening protocols. *J Med Chem* **48:**5448–5465.

Evers A and Klabunde T (2005) Structure-based drug discovery using GPCR homol-

ogy modeling: successful virtual screening for antagonists of the alpha1A adrenergic receptor. *J Med Chem* **48:**1088–1097.
Gomella L and Haist S (2004) *Clinician's Pocket Drug Reference 2004.* McGraw-Hill, Columbus, OH.
Goodwin B, Moore LB, Stoltz CM, McKee DD, and Kliewer SA (2001) Regulation of the human CYP2B6 gene by the nuclear pregnane X receptor. *Mol Pharmacol* **60:**427–431.
Gupta D, Venkatesh M, Wang H, Kim S, Sinz M, Goldberg GL, Whitney K, Longley C and Mani S (2008) Expanding the roles for pregnane X receptor (PXR) in cancer: proliferation and drug resistance in ovarian cancer. *Clin Cancer Res*, in press.
Healan-Greenberg C, Waring JF, Kempf DJ, Blomme EA, Tirona RG, and Kim RB (2008) HIV protease inhibitor A-792611 is a novel functional inhibitor of human PXR. *Drug Metab Dispos* **36:**500–507.
Hopkins AL, Groom CR, and Alex A (2004) Ligand efficiency: a useful metric for lead selection. *Drug Discov Today* **9:**430–431.
Huang H, Wang H, Sinz M, Zoeckler M, Staudinger J, Redinbo MR, Teotico DG, Locker J, Kalpana GV, and Mani S (2007) Inhibition of drug metabolism by blocking the activation of nuclear receptors by ketoconazole. *Oncogene* **26:**258–268.
Hurst CH and Waxman DJ (2004) Environmental phthalate monoesters activate pregnane X receptor-mediated transcription. *Toxicol Appl Pharmacol* **199:**266–274.
Johnson DR, Li CW, Chen LY, Ghosh JC, and Chen JD (2006) Regulation and binding of pregnane X receptor by nuclear receptor corepressor silencing mediator of retinoid and thyroid hormone receptors (SMRT). *Mol Pharmacol* **69:**99–108.
Jones G, Willett P, Glen RC, Leach AR, and Taylor R (1997) Development and validation of a genetic algorithm for flexible docking. *J Mol Biol* **267:**727–748.
Kalgutkar AS, Nguyen HT, Vaz AD, Doan A, Dalvie DK, McLeod DG, and Murray JC (2003) In vitro metabolism studies on the isoxazole ring scission in the anti-inflammatory agent leflunomide to its active α-cyanoenol metabolite A771726: mechanistic similarities with the cytochrome P450-catalyzed dehydration of aldoximes. *Drug Metab Dispos* **31:**1240–1250.
(Kliewer SA, Moore JT, Wade L, Staudinger JL, Watson MA, Jones SA, McKee DD, Oliver BB, Willson TM, Zetterström RH, et al. (1998) An orphan nuclear receptor activated by pregnanes defines a novel steroid signalling pathway. *Cell* **92:**73–82.
Krasowski MD, Yasuda K, Hagey LR, and Schuetz EG (2005) Evolution of the pregnane X receptor: adaptation to cross-species differences in biliary bile salts. *Mol Endocrinol* **19:**1720–1739.
Leach AR, Shoichet BK, and Peishoff CE (2006) Prediction of protein-ligand interactions. Docking and scoring: successes and gaps. *J Med Chem* **49:**5851–5855.
Lemaire G, Benod C, Nahoum V, Pillon A, Boussioux AM, Guichou JF, Subra G, Pascussi JM, Bourguet W, Chavanieu A, et al. (2007) Discovery of a highly active ligand of human pregnane X receptor: a case study from pharmacophore modeling and virtual screening to "in vivo" biological activity. *Mol Pharmacol* **72:**572–581.
Mani S, Huang H, Sundarababu S, Liu W, Kalpana G, Smith AB, and Horwitz SB (2005) Activation of the steroid and xenobiotic receptor (human pregnane X receptor) by nontaxane microtubule-stabilizing agents. *Clin Cancer Res* **11:**6359–6369.
Moore LB, Parks DJ, Jones SA, Bledsoe RK, Consler TG, Stimmel JB, Goodwin B, Liddle C, Blanchard SG, Willson TM, et al. (2000) Orphan nuclear receptors constitutive androstane receptor and pregnane X receptor share xenobiotic and steroid ligands. *J Biol Chem* **275:**15122–15127.
Reynolds CH, Tounge BA, and Bembenek SD (2008) Ligand binding efficiency: trends, physical basis, and implications. *J Med Chem* **51:**2432–2438.
Rozman B (2002) Clinical pharmacokinetics of leflunomide. *Clin Pharmacokinet* **41:**421–430.
Schapira M, Abagyan R, and Totrov M (2003a) Nuclear hormone receptor targeted virtual screening. *J Med Chem* **46:**3045–3059.
Schapira M, Raaka BM, Das S, Fan L, Totrov M, Zhou Z, Wilson SR, Abagyan R, and Samuels HH (2003b) Discovery of diverse thyroid hormone receptor antagonists by high-throughput docking. *Proc Natl Acad Sci U S A* **100:**7354–7359.
Schapira M, Raaka BM, Samuels HH, and Abagyan R (2000) Rational discovery of novel nuclear hormone receptor antagonists. *Proc Natl Acad Sci U S A* **97:**1008–1013.
Schapira M, Raaka BM, Samuels HH, and Abagyan R (2001) In silico discovery of novel retinoic acid receptor agonist structures. *BMC Struct Biol* **1:**1.
Schuetz E and Strom S (2001) Promiscous regulator of xenobiotic removal. *Nature medicine* **7:**536–537.
Synold TW, Dussault I, and Forman BM (2001) The orphan nuclear receptor SXR coordinately regulates drug metabolism and efflux. *Nat Med* **7:**584–590.
Tabb MM, Kholodovych V, Grün F, Zhou C, Welsh WJ, and Blumberg B (2004) Highly chlorinated PCBs inhibit the human xenobiotic response mediated by the steroid and xenobiotic receptor (SXR). *Environ Health Perspect* **112:**163–169.
Ung CY, Li H, Yap CW, and Chen YZ (2007) In silico prediction of pregnane X receptor activators by machine learning approaches. *Mol Pharmacol* **71:**158–168.
Wang CY, Li CW, Chen JD, and Welsh WJ (2006) Structural model reveals key interactions in the assembly of the pregnane X receptor/corepressor complex. *Mol Pharmacol* **69:**1513–1517.
Wang H, Huang H, Li H, Teotico DG, Sinz M, Baker SD, Staudinger J, Kalpana G, Redinbo MR, and Mani S (2007) Activated PXR is a target for ketoconazole and its analogs. *Clin Cancer Res* **13:**2488–2495.
Wang H, Li H, Moore LB, Johnson MD, Maglich JM, Goodwin B, Ittoop OR, Wisely B, Creech K, Parks DJ, et al. (2008) The phytoestrogen coumestrol is a naturally occurring antagonist of the pregnane X receptor. *Mol Endocrinol* **22:**838–857.
Watkins RE, Davis-Searles PR, Lambert MH, and Redinbo MR (2003) Coactivator binding promotes the specific interaction between ligand and the pregnane X receptor. *J Mol Biol* **331:**815–828.
Watkins RE, Maglich JM, Moore LB, Wisely GB, Noble SM, Davis-Searles PR, Lambert MH, Kliewer SA, and Redinbo MR (2003b) 2.1Å crystal structure of human PXR in complex with the St John's Wort compound hyperforin. *Biochemistry* **42:**1430–1438.
Watkins RE, Noble SM, and Redinbo MR (2002) Structural insights into the promiscuity and function of the human pregnane X receptor. *Curr Opin Drug Discov Devel* **5:**150–158.
Watkins RE, Wisely GB, Moore LB, Collins JL, Lambert MH, Williams SP, Willson TM, Kliewer SA, and Redinbo MR (2001) The human nuclear xenobiotic receptor PXR: structural determinants of directed promiscuity. *Science* **292:**2329–2333.
Xue Y, Chao E, Zuercher WJ, Willson TM, Collins JL, and Redinbo MR (2007a) Crystal structure of the PXR-T1317 complex provides a scaffold to examine the potential for receptor antagonism. *Bioorg Med Chem* **15:**2156–2166.
Xue Y, Moore LB, Orans J, Peng L, Bencharit S, Kliewer SA, and Redinbo MR (2007b) Crystal structure of the pregnane X receptor-estradiol complex provides insights into endobiotic recognition. *Mol Endocrinol* **21:**1028–1038.
Zhang T, Zhou JH, Shi LW, Zhu RX, and Chen MB (2007) 3D-QSAR studies with the aid of molecular docking for a series of non-steroidal FXR agonists. *Bioorg Med Chem Lett* **17:**2156–2160.
Zhou C, Poulton EJ, Grün F, Bammler TK, Blumberg B, Thummel KE, and Eaton DL (2007) The dietary isothiocyanate sulforaphane is an antagonist of the human steroid and xenobiotic nuclear receptor. *Mol Pharmacol* **71:**220–229.

Address correspondence to: Dr. Sean Ekins, Collaborations in Chemistry, Jenkintown, PA 19046. E-mail: ekinssean@yahoo.com